Investigation of solvated calcium dication structure in pure water, methanol, and ethanol solutions by means of K and L2,3-edges X-ray absorption spectroscopy

Thanit Saisopa, Kanchanasuda Klaiphet, Prayoon Songsiriritthigul, Wandared Pokapanich, Saowanaporn Tangsukworakhun, Chomphunuch Songsiriritthigul, Chatree Saiyasombat, Yuttakarn Rattanachai, Hayato Yuzawa, Nobuhiro Kosugi, et al.

Investigation of solvated calcium dication structure in pure water, methanol, and ethanol solutions by means of K and $L_{2,3}$-edges X-ray absorption spectroscopy

*Thanit Saisopa [1,2], Kanchanasuda Klaiphet [1,2], Prayoon Songsiriritthigul [1,2], Wandared Pokapanich [3], Saowanaporn Tangsukworakhun [3], Chomphunuch Songsiriritthigul [4], Chatree Saiyasombat [4], Yuttakarn Rattanachai [5], Hayato Yuzawa [6], Nobuhiro Kosugi [6], Denis Céolin [7]**

[1] Research Network NANOTEC–SUT on Advanced Nanomaterials and Characterization, School of Physics, Suranaree University of Technology, Nakhon Ratchasima 30000, Thailand

[2] Thailand Center of Excellence in Physics, Ministry of Higher Education, Science, Research and Innovation, Bangkok 10400, Thailand

[3] Faculty of Sciences, Nakhon Phanom University, Nakhon Phanom, 48000, Thailand

[4] Synchrotron Light Research Institute, Nakhon Ratchasima, 30000, Thailand

[5] Department of Applied Physics, Faculty of Sciences and Liberal Arts, Rajamangala University of Technology Isan, Nakhon Ratchasima 30000, Thailand

[6] UVSOR-III Synchrotron, Institute for Molecular Science, Myodaiji, Okazaki 444-8585, Japan

[7] Synchrotron SOLEIL, l'Orme des Merisiers, Saint-Aubin, F-91192 Gif-sur-Yvette Cedex, France

Abstract

The interaction of an ion with surrounding solvent molecules is revealed by X-ray absorption spectroscopy in transmission mode for the case of calcium dication dissolved in pure water, methanol and ethanol at the Ca K and $L_{2,3}$-edges. The near-threshold K-shell excitation leads to two distinct solvent-dependent features, the Ca 1s to 3d and 4p electronic transitions, clearly indicating the ligand field decreases as water is changed to methanol and methanol to ethanol. On the other hand, the Ca $L_{2,3}$-edge excitation leads to small changes in the absorption spectra and the peak assignment – mostly in terms of Ca 2p to e_g and t_{2g} transitions for each of the two spin orbit components – is strongly depending on the geometry of the first solvation shell around the dication and on the magnitude of the ligand-field multiplet effects. Our interpretation is supported by ab-initio quantum chemical calculations of the solvent dependence of chemical shifts for the Ca 3d and 4p unoccupied levels of the 1s and 2p excited states, performed on a small cluster including the nearest neighbor solvent molecules surrounding the Ca dication assuming a cubic (8-fold) solvent coordination.

Introduction:

Numerous theoretical and experimental methods have been applied for the determination of the structural parameters defining the local organization within an electrolyte solution. These intensive studies are motivated by the need of modeling and understanding – at the fundamental level – the interaction of an ion with surrounding solvent molecules, and also by the crucial role of some hydrated ions in many biochemical processes occurring in living organisms. In this context, the Ca^{2+} ion has been frequently investigated due to its abundance in human body and its participation in e.g. signal transduction, blood coagulation as well as muscle contraction. Knowing the local structure in Ca^{2+} aqueous solutions is thus one of the elementary steps necessary for a proper description of the chemical reactions in which it is involved.

The coordination number of an ion and the structure of its solvation shell can be investigated experimentally by various methods including X-ray absorption fine structure (XAFS) and X-ray diffraction (XRD). These techniques have advantages and disadvantages, and are complementary as demonstrated e.g. in reference.[1] XRD is well adapted to probe the long-range structure in crystalline samples. However, applied to disordered systems the data deconvolution procedures usually lack of precision to extract clear short-range contributions. On the contrary, XAFS, in addition of being chemically selective, is an efficient probe of the surrounding effect of the targeted element. The rather small kinetic energy of the emitted core photoelectron leads to a short inelastic mean free path that reduces the probability of being scattered by distant atoms, but favors multiple scattering from neighboring ones. Adapted to electrolyte solutions, this allows to determine the solvent organization near a selected atomic ion and the local solvent arrangement such as symmetry and coordination number of the first shell from the excitation close to the

corresponding core-ionization edge. Another advantage of the X-ray absorption method is its ability of probing samples on a large concentration range due to a high sensitivity of the ion-solvent pair distribution function, whereas XRD is efficient mostly for highly concentrated solutions.

In the case of Ca^{2+} placed in an aqueous environment, several experimental reports based on either of these two methods suggest average coordination numbers between 6 and 8 water molecules in the first solvation shell, for Ca-O bond lengths going from 2.39 to 2.46 Å. These values are obtained on a rather large concentration range going from about 0.1M up to 6M, with different types of salts, i.e. with Cl^-, Br^-, I^- or $(NO_3)^{2-}$ as counter ions. Theoretical treatments with Car-Parinello and Monte-Carlo methods give similar values for the coordination number, whereas classical and quantum molecular dynamics lead to slightly larger values, i.e. between 8 and 10 water molecules for similar average bond lengths [cf e.g. references[2-4] and summary in Table 1. of reference[5]].

The effect of salt concentration on the hydrated calcium structure was also investigated at several instances [see e.g. references[6-9]]. There are only a few references in which the role of the solvent on the structure of the solvated calcium dication is explored. One of them is a study performed by Kim[10] by means of Monte Carlo simulations and another one is done by Megyes et al., [5] by combining ab-initio quantum chemical calculations and XRD experiments. These two references are in adequacy with the structural properties of the hydrated calcium dication as given previously. For the methanol solvent, Kim obtained theoretical values of 7 first neighbors located at a bond length of 2.3 Å from Ca^{2+} (to be compared with the values 8 and 2.4 Å for the water solvent with the same theoretical method), whereas Megyes et al. obtained for a 1M solution, the values of 6 first neighbors at a bond length of 2.39 Å from Ca^{2+} (to be compared

with 8 and 2.46 Å for water with the same method at the same concentration). To our knowledge, no information describing the structural properties of the calcium dication solvated in ethanol is available.

In this article we present the X-ray absorption spectra of Ca^{2+} recorded in the vicinity K- and $L_{2,3}$-shells ionization thresholds, for calcium chloride salt dissolved in 3 different polar solvents, namely water, methanol and ethanol. In the specific case of the Ca K-edge excitation, there are some discrepancies in the interpretation of the first features located in the vicinity of the 1s ionization threshold, since they are not unambiguously attributed to specific transitions (i.e. 1s to 4s in references 11 and 12, and 1s to 4p in references 6 and 7). On the other hand, for the Ca $L_{2,3}$-edge excitation spectra obtained in such liquid media, their interpretation has been based on that obtained on solid samples. To support our interpretation of the full set of data recorded at 2 different edges for 3 different solvation cases, we have applied a single ab-initio quantum chemical model. A consistent picture of the calcium nearest neighbor structure is shown by disentangling the contributions of the different excited orbitals involved in these transitions.

Experiments:

Soft X-ray absorption measurements were performed at the BL3U beamline, UVSOR-III Synchrotron, Institute for Molecular Science (IMS), Japan. This beamline covers the 60-800 eV photon energy range and a resolving power of $\Delta E/E=10^{-4}$ is achieved by means of a varied-line-spacing plane grating monochromator[13]. The spectra were recorded in transmission mode using a special liquid flow cell whose thickness is optimized by a controlled He pressure inside a dedicated vacuum chamber. A full description of the corresponding setup is given in the article

of M. Nagasaka et al., [14]. Photon energy calibration was done using the known N1s XAS of a polymer film as described in this last reference.

Hard X-ray absorption measurements were performed at the BL1.1W beamline at the Synchrotron Light Research Institute of Thailand, which covers the 4-18keV photon energy range and achieves a resolving power $\Delta E/E=10^{-4}$ by means of a Si(111) double crystal monochromator [15]. The spectra were recorded in a partial fluorescence mode with a commercial Canberra 19-element Ge solid-state detector. Photon energy calibration was done using a solid sample of $CaCO_3$.

For both experiments, XAS measurements of the empty cells in the vicinity of the calcium K- and $L_{2,3}$-shells ionization thresholds were performed to remove undesirable contaminations in the spectrum.

Calcium chloride salt is dissolved in several polar solvents. The choice of the concentration was motivated by three main arguments. The first one is related to the possible formation of ion pairs that we would reduce as much as possible in order to focus on the description of the calcium dication surrounded only by solvent molecules. This implies in principle to work at low concentration. The second one is correlated to the solubility of this salt in the methanol and ethanol solvent, determined at 29.2g/100g and 25.8g/100g at 20°C respectively, which sets an upper-limit value. A last argument concerns the intensity of the XAS signal collected during the two distinct experimental sessions, where we would like to get intensities large enough due to limited amount of time. We determined a concentration of 0.5M for each solution as a good compromise.

Theoretical Methods:

The present quantum chemical calculations were carried out to understand the experimental results of the solvent dependence of chemical shifts for the Ca 3d and 4p unoccupied levels in the 1s and 2p excited states. The nearest neighbor Ca-O coordination geometry of solvent molecules, water, methanol, and ethanol, was assumed in the cubic symmetry with 8 solvent molecules around Ca^{2+} ion and was optimized within such a small cluster model. There should be many other possibilities for local coordination geometries around Ca^{2+}; however, the choice of 8 molecules is a good compromise since we could expect a value of a little more than 8 for the water case, and a value of a little less than 8 for methanol and ethanol cases, considering the information collected in the literature[5]. To support this approximation, our measurements are compared with similar published Ca K-edge and $L_{2,3}$-edge XAFS spectra (as discussed later), which allows us to assume the 3d e_g lower in energy than 3d t_{2g} with comparable 10Dq (i.e. $\Delta E(e_g - t_{2g})$).

The coordination number is correlated to the Ca-O bond length (with a negative oxygen atom being the nearest neighbor to the positively charged calcium atom); that is, the smaller coordination number causes the smaller Ca-O bond length. Even if so, the total ligand field should not be so different, considering similar Ca K-edge and $L_{2,3}$-edge XAFS spectra. Therefore, in the present cluster model, we calculated a model of 8 solvent molecules with the same Ca-O bond length in the cubic symmetry.

To compare the experimental spectra with the final excited states, the orbital relaxation in presence of a core vacancy, 1s or 2p, is explicitly considered under the Hartree-Fock self-consistent-field (HF-SCF) approximation for a restricted doublet open-shell state. Ca 1s excitations are evaluated by the static exchange (STEX) or hole potential method.[16] The 2p core orbitals were obtained from the 2s core hole solution.[17] Spin-orbit interaction for 2p excitations

is taken into account within the Breit-Pauli approximation.[17,18] The basis sets of the calcium, carbon and oxygen, and hydrogen atoms are of (211213/21121), (721/7), and (6) contractions [19], and are augmented with two Ca 3p (ζ=0.069, 0.023) and four 3d (ζ=4.182, 1.308, 0.397, 0.108) functions. All the calculations were carried out by using the GSCF3 program package. [20, 21]

Results and Discussion:

Ca K-edge XAFS:

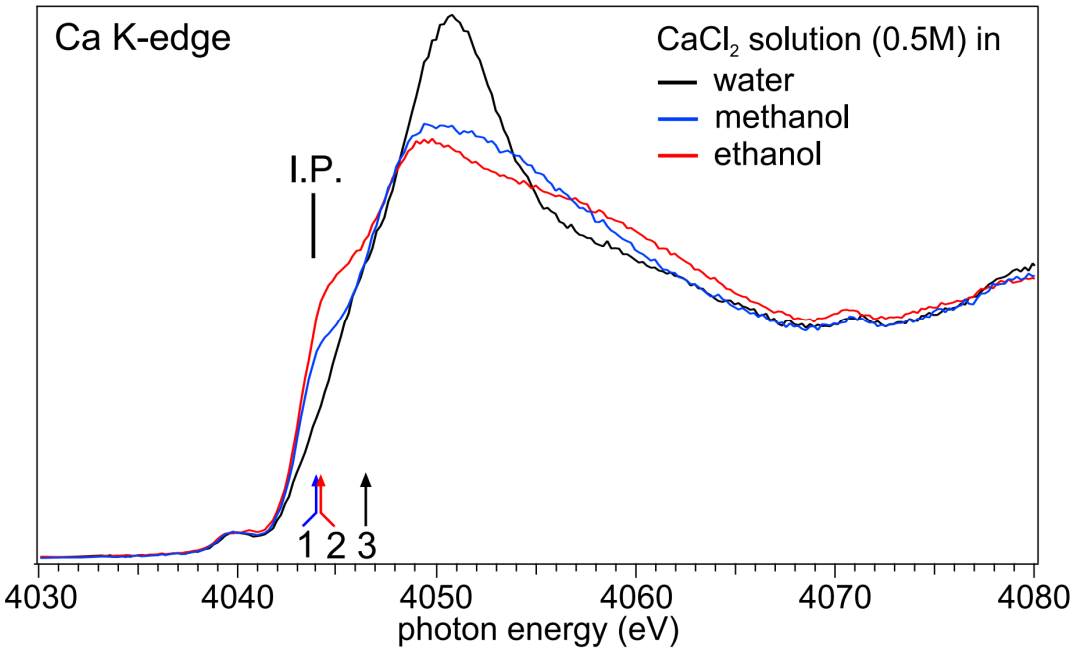

Figure 1: X-ray absorption spectra of solutions of $CaCl_2$ salt diluted in water (black), methanol (blue), and ethanol (red), at a concentration of 0.5M, recorded in the vicinity of the Ca^{2+} K-shell ionization threshold. The spectra are normalized on the maximum of the Ca 1s to 3d transition at about 4040 eV photon energy. The arrows labelled 1, 2 and 3 correspond to the position of the excitonic features. The attribution of the different structures is given in the text.

In Figure 1 we present the X-ray absorption spectra recorded in the vicinity of the 1s orbital ionization potential of the solvated calcium dication. The solvents are water (black curve), methanol (blue curve) and ethanol (red curve). All the three solutions have a concentration of 0.5M. The hydrated XAFS spectrum published in e.g. references,[2,7] are comparable with the

present one. Around 4040 eV photon energy, a pre-edge structure is attributed to the dipole-forbidden electronic transition Ca 1s to 3d, as discussed below (cf Figure 2). For Fulton et al.,[6, 7] this transition is forbidden for octahedral symmetries but is either quadrupolar-allowed, or populated due to thermal disorder and vibronic coupling inducing some p-character in the excited state configuration leading to a small structure. The second and main peak is large and its maximum position is located at 4050.8 eV photon energy for the aqueous solution, above the corresponding Ca 1s ionization threshold located at 4043.6 eV (this value is obtained by XPS measurements and will be described in a forthcoming paper [22]). For the methanol and ethanol cases, the main peak position is located at about 4050 eV and 4049.6 eV respectively. A third resonance located at about 4071 eV for all samples is attributed to "doubly excited states" excitation whose configuration corresponds to the ionization of the Ca 1s orbital plus an electron shake from the outermost occupied orbital to the lowest unoccupied one. Between the second and third resonance there is a structureless region centered at 4060 eV photon energy that is changing in intensity depending on the solvent. The structures observed near 4045 eV photon energy and associated with the arrows labelled 1, 2 and 3 will be discussed in the following.

Below the threshold, the 1s to 3d region displays small intensity variations as a function of the solvent (see Figure 2). From a broad and seemingly single structure centered at 4040 eV for the water case, we discern a potential double structure for the ethanol case with one maximum at 4039.4 eV and a second one at 4040.6 eV. For methanol the situation is intermediate, and we observe a main peak having a maximum at 4039.8 eV, and a smaller structure that seems centered at 4040.6 eV.

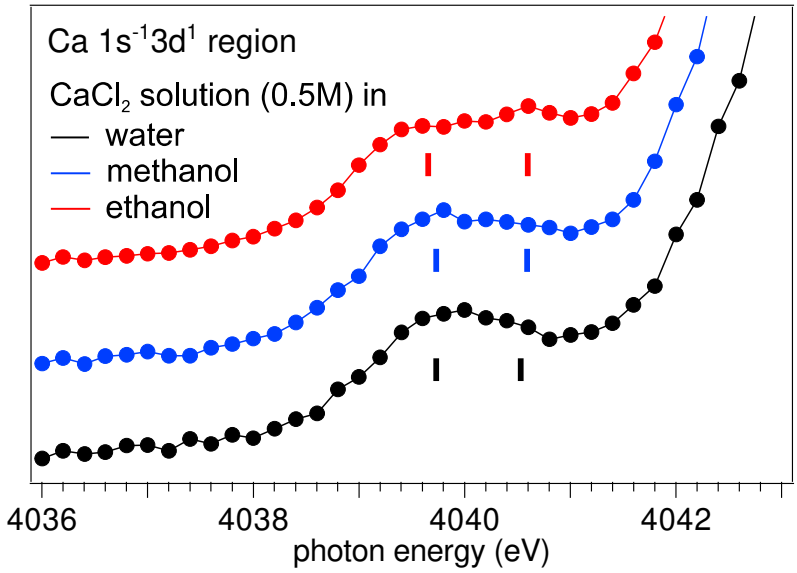

Figure 2: Pre-edge X-ray absorption spectra of solutions of $CaCl_2$ salt diluted in water (black), methanol (blue), and ethanol (red), at a concentration of 0.5M. Colored vertical bars refer to the energy positions of e_g and t_{2g} orbitals calculated for each solvent, in the case of a cubic (8-fold) coordination using the optimized Ca-O bond length as obtained in Table 1.

These variations are attributed to different splitting values of the 3d orbitals under the crystal field effects generated by the solvent molecules around the calcium dication. In table 1 we summarize the results of the calculations performed assuming a cubic (8-fold) oxygen coordination around calcium, for different Ca-O bond lengths depending on the solvent. The Ca 1s to e_g and t_{2g} excitations are obtained in terms of relative energy to the ionization threshold:

Solvent	Ca-O bond length	e_g	t_{2g}	ΔE

Water	2.44 Å (optimized)	-11.79 eV	-10.99 eV	0.80 eV
Methanol	2.51 Å (optimized)	-12.03 eV	-11.17 eV	0.86 eV
Ethanol	2.60 Å (optimized)	-12.45 eV	-11.51 eV	0.94 eV
Water	2.60 Å (fixed)	-11.24 eV	-10.30 eV	0.94 eV
Methanol	2.60 Å (fixed)	-12.50 eV	-11.57 eV	0.93 eV
Ethanol	2.60 Å (fixed)	-12.45 eV	-11.51 eV	0.94 eV

Table 1: Average energy positions of e_g and t_{2g} orbitals calculated for each solvent, in the case of a cubic (8-fold) coordination using the optimized and fixed (to 2.60 Å) Ca-O bond length. The energy is shown relative to the calculated Ca 1s ionization potential.

The absolute position of the resonances relative to the Ca 1s ionization potential calculated is over estimated due to the model calculated without counter ions (anions) in a totally neutral system. However, the $\Delta E(e_g - t_{2g})$ value obtained in this calculation (0.8 to 0.94 eV), is in adequacy with our measurements. In addition, and for this specific geometry, the variation of the $e_g - t_{2g}$ energy splitting is correct, i.e. slightly larger for ethanol than for water, methanol being an intermediate situation. Furthermore, to evaluate potential ligand effects, we performed calculations in this geometry at a fixed Ca-O bond length of 2.6 Å. It results that the e_g and t_{2g} energy positions do not change noticeably from the ethanol case presented in Table 1, leading to an almost constant energy splitting of 0.94 eV. The $\Delta E(e_g - t_{2g})$ of water and methanol increase for the longer Ca-O bonds. This is because the e_g and t_{2g} orbitals are not completely degenerate and their energy broadenings (0.1-0.2 eV) decrease in the longer Ca-O bond. We should notice

that in an octahedral (6-fold) coordination, the energetic order of the split 3d orbitals will dramatically change, that is the t_{2g} component becomes energetically lower than the e_g one, and that a modification of the solvation geometry could also lead to different splitting values. However, an estimate of the energy position and intensity of these components for several cluster geometries goes beyond the scope of the present article.

Above the onset of the ionization threshold, the general shape of the Ca K-edge spectra is also largely dependent on the type of solvent, which might influence the ion coordination number and associated symmetries (see e.g.[6,23-24]). Interestingly, the structure of the main peak is not unambiguously attributed even for the water case. For systems with only water in the first coordination shell, Fulton et al.[6], assigned the intense main structure near 4050 eV to a large oscillation resulting from the Ca-O single scattering in the first hydration shell, with weaker multiple scattering in the first shell as well as second shell single scattering contributions. A closer look at the water-related curve presented in Figure 1 indicates the presence of a very small shoulder on the low photon energy side of the main peak, at about 4046.5 eV (arrow 3). For methanol and ethanol this shoulder is much more prominent and is shifted toward lower photon energy values at 4044 eV (arrow 1) and 4044.2 eV (arrow 2) respectively. Still in reference 6, the XAFS spectrum corresponding to the very diluted species 0.2m of $Ca(ClO_4)_2$ in water is nearly identical to the one of the aqueous Ca^{2+} solution presented in Figure 1, and these shoulders are attributed to Ca 1s to 4p transitions. However, instead of these attributions, other publications showing results only on solid samples indicate that the main peak is attributed to the Ca 1s to $4p_{1/2, 3/2}$ transitions whereas the low-energy shoulder is assigned to the Ca 1s to 4s quadrupolar transition[11,12].

By analogy with the work of Kosugi et al.[25] on copper compounds, most contributions from dipole-allowed Ca 1s to 4p transitions with strong crystal fields appear above the ionization threshold but some excitonic bound-state 4p features with weak crystal fields appear below the threshold. Table 2 shows the energy positions of these Ca 4p excitonic features, calculated assuming a cubic (8-fold) coordination around Ca^{2+}. In the case of optimized Ca-O bond length for each solvent (Table 2, upper half part), calculations predict that the pre-edge 4p excitonic feature is more prominent and is more shifted to lower energy for the solvent having longer a Ca-O bond length.

Solvent	Ca-O bond length	lower 4p	higher 4p	ΔE	Oscillator strength (f)	
Water	2.44 Å (optimized)	-2.84 eV	-2.06 eV	0.78 eV	0.00050	0.00053
Methanol	2.51 Å (optimized)	-4.70 eV	-3.38 eV	1.32 eV	0.00051	0.00070
Ethanol	2.60 Å (optimized)	-6.18 eV	-4.75 eV	1.43 eV	0.00081	0.00090
Water	2.60 Å (fixed)	-3.86 eV	-3.20 eV	0.66 eV	0.00091	0.00097
Methanol	2.60 Å (fixed)	-6.65 eV	-4.80 eV	1.85 eV	0.00076	0.00086
Ethanol	2.60 Å (fixed)	-6.18 eV	-4.75 eV	1.43 eV	0.00081	0.00090

Table 2: Energy positions of Ca 4p excitonic features calculated for each solvent in the case of a cubic (8-fold) coordination using the optimized and fixed (to 2.60 Å) Ca-O bond length. The energies are shown relative to the calculated Ca 1s ionization potential. The corresponding oscillator strengths are also shown.

In the liquid the symmetry is distorted and the three 4p excitations are not degenerate as for the assumed cubic (8-fold) coordination around the Ca dication. This is not applicable to the 3d case as shown in Table 1, where the 3d are not so sensitive to the distortion or does not show any mixing with 4p. This difference can be explained by the different radial distribution of the 3d and 4p; that is, 4p are more diffuse and are much more sensitive to other atoms beyond the nearest neighbor O atom. This result is in qualitative agreement with the present experiment since the excitonic 4p features are measured more intense for ethanol than methanol due to the larger Ca-O bond length or the weaker O ligand field in ethanol. If the Ca-O coordination distance is the same, a coordination number larger than 8 could make the 4p state energy closer to the ionization threshold (calculated at higher energy) and the 4p feature invisible. On the other hand, a coordination number smaller than 8 could make the pre-edge excitonic 4p state more intense and clearly observed.

Ca $L_{2,3}$ edge XAFS:

To our knowledge, there is no published X-ray absorption spectrum of solvated calcium dication recorded in the vicinity of the Ca 2p ionization potential. However, various calcium compounds have been studied in the past, either in powder form[26], deposited on surface,[27-29] or as single-crystal or thin-film sample[30]. Theoretically, X-ray absorption spectra of d^0 compounds were calculated for the $2p^63d^0$ to $2p^53d^1$ excitation, using first an atomic multiplet description of the corresponding states and then by applying on them the crystal field effect[31]. Despite some small discrepancies, this method leads to excellent agreements with the experimental results obtained on bulk CaF_2. In addition of being quantitatively efficient, this approach allowed explaining the origin of small features that the authors attribute to either surfaces or interfaces

effects, observed in addition of the main bulk contribution[32]. These weaker contributions were the subject of partly contradictory attributions (cf. reference[28] and corresponding replies in[30-33]). Different methods were then applied to simulate the $L_{2,3}$ edge X-ray absorption spectra of calcium for the CaO and CaF_2 compounds, as the multichannel multiple scattering theory (MCMS)[34] and the configuration interaction (CI)[35]. In this latter reference, Ca 2p to 3d spectra are well reproduced by assuming the cubic (8-fold) coordination, but not the octahedral (6-fold) coordination.

Previously in the introduction, the values of the coordination numbers found in the literature for the hydrated calcium case were presented and they vary mostly between 6 and 8 independently of the experimental or theoretical methods used. Comparatively, the symmetry in the simulations presented in the reference[36] is octahedral in the case of the CaO structure, with a 6-fold coordination for Ca, and cubic in the case of CaF_2, with a 8-fold coordination for Ca. The simulations for both systems lead to 10Dq values of opposite signs, (positive for CaO, negative for CaF_2) leading to opposite e_g - t_{2g} orbital energy ordering. In the following we will use the $a_{1,2}/b_{1,2}$ notation that was given in the references[31, 35-36] for the description of our spectra.

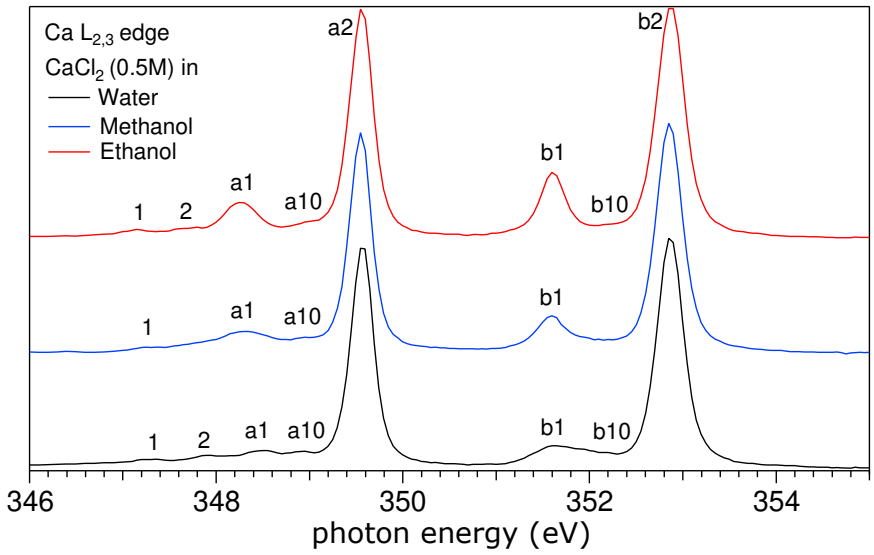

Figure 3: X-ray absorption spectra of solutions of $CaCl_2$ salt diluted in water (black), methanol (blue), and ethanol (red), at a concentration of 0.5M, recorded in the vicinity of the Ca^{2+} $L_{2,3}$ ionization thresholds. The spectra are normalized on the maximum of the transition located at about 353 eV photon energy. The attribution of the different structures is given in the text.

In Figure 3, we present the Ca^{2+} $L_{2,3}$ X-ray absorption spectra of solutions of $CaCl_2$ diluted in water, methanol and ethanol at a concentration of 0.5M, normalized on the maximum intensity of the main peak. The peak positions, when available, are summarized in Table 3.

Solvent	1	2	a_1	a_{10}	a_2	b_1	b_{10}	b_2
Water	347.3	347.9	348.45	348.9	349.56	351.6	352.17	352.86
Methanol	347.25		348.32	348.95	349.56	351.6		352.86
Ethanol	347.12	347.7	348.27	349	349.56	351.6	352.2	352.86

Table 3: Peak positions (in eV) of the Ca^{2+} $L_{2,3}$ XAS spectra for the 3 solvents, as observed in Figure 3.

We can see that the two spin-orbit split contributions (region ~346<hν<350.5 eV for L_3, and ~350.5<hν<355 eV for L_2), have each a main line a_2 at 349.56 eV and b_2 at 352.86 eV, whose energy position do not change with the solvent, and at least a smaller one a_1 at 348.45 eV (water), 348.32 eV (methanol), 348.27 eV (ethanol), and b_1 at 351.6 eV (for the 3 solvents). The separation a_2-b_2 corresponds to the $2p_{3/2}$-$2p_{1/2}$ spin-orbit splitting and the peak separation (a_1-a_2) and (b_1-b_2) is related to the crystal-field effect. The small a_1/a_2 and b_1/b_2 intensity ratios are an indication of a small crystal field 10Dq value. We note that the b_1 structure is strongly asymmetric for water and to a less extend for methanol, suggesting a superposition of several states. Two smaller leading peaks (named 1 and 2 in Figure 3 and Table 1) visible in the region below 348 eV are determined as being part of the $2p^53d^1$ multiplet and their positions is mostly governed by the exchange interaction.[18] The crystal-field effect does not influence their position and intensity notably. This goes in line with our measurements since we do not observe a clear dependence on the solvent. In between the main peaks (a_1 and a_2, and b_1 and b_2), we measure small features (a_{10} and b_{10}) near 349 eV and 352.2 eV for the 3 solvents. These were discussed in the references[27-28, 31-32, 36] and could possibly originate from the contribution of monovalent Ca^+ ion having an extra 4s electron in its ground state configuration, and whose corresponding absorption spectrum ($2p^63d^04s^1$ to $2p^53d^14s^1$), much weaker in intensity than the main one, is shifted to lower energy.

The data in Figure 3 are normalized on the maximum intensity of the main peak b_2 located at about 353 eV. With this normalization, all a_2 peaks have almost the same maximum value. The

global shape of the spectrum associated with the water solvent differs slightly from the two others. However, a closer inspection shows that the three spectra seem to follow a trend along the series water→methanol→ethanol, in which the a_1 and b_1 peaks become more intense and converge to the photon energy values of 348.27 eV and 351.6 eV respectively.

Our present theoretical calculations of the Ca-O bond length dependence of Ca^{2+} with cubic 8-fold water coordination predict the shorter bond length reduces the relative a_1 and b_1 bands intensities (corresponding to the e_g components in this geometry, a_2 and b_2 bands arising mostly from the t_{2g} components) as shown in Figure 4. Except for the a_1 and a_2 and b_1 and b_2 regions, there are too many states with weak 2p-3d components and the simulated spectra are not compatible to the experiment. More reliable calculations are necessary to simulate all the spectral region.

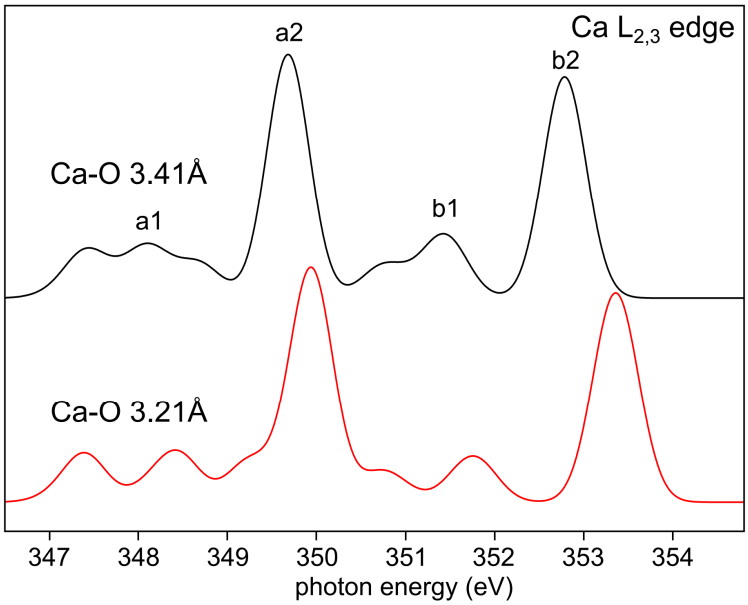

Figure 4: Simulated Ca $L_{2,3}$-edge X-ray absorption spectra in a cubic 8-fold water coordination illustrating the influence of the Ca-O bond length on the a_1/a_2 and b_1/b_2 intensity ratio.

If this result can be applied to methanol and ethanol solutions, a_1 and b_1 peaks should be more prominent in ethanol – as observed. Furthermore, the higher coordination number than 8 molecules or the shorter coordination distance is expected to cause an increase in energy difference between e_g-type lower (less anti-bonding) states and t_{2g}-type higher (more anti-bonding) states. On the other hand, the smaller coordination number like 6 in the O_h symmetry causes a completely different picture where the 3d-t_{2g} is lower than 3d-e_g. This interpretation is almost consistent with the following comparison of the solvated Ca case with some calcium-based compounds of known structures.

Comparison with other Ca compounds:

The summary of several studies presented in the Table 1 of Megyes et al. article[5] illustrates the variety of results available on the structural parameters of the solvation shell of Ca^{2+} in water or methanol, based on different methods of investigation.

We can also make a parallel between our work and the one of Fulton et al.[6], in which the role of the Ca^{2+} environment on the shape of the XAFS spectra taken near the Ca 1s ionization threshold and for different types of samples was probed. In their work, the principal modifications observed by changing the calcium near structure concern the position and intensity of the main peak and of the shoulder that it attributed to the Ca 1s to 4p transition. As previously discussed, the spectrum of the low concentrated 0.2m of $Ca(ClO_4)_2$ aqueous solution is nearly identical to the one we present in Figure 1 and related to the water solvent. At higher concentration, the 6.0m hydrated $CaCl_2$ spectrum exhibits a more intense shoulder and a less intense main peak, which is slightly shifted toward lower photon energy. The presence of Cl^- ion

in the second solvation shell is invoked to explain such difference. The $CaCl_2 6(H_2O)$ solid spectrum is somehow similar to the one corresponding with the highly concentrated $CaCl_2$ aqueous solution, with a shoulder even more intense and a main peak more shifted toward lower energy and slightly less intense. Then the two other solid samples, $CaCl_2 2(H_2O)$ and $CaCl_2$, look rather similar, with the shoulder becoming intense and the main peak being largely shifted to the low photon energy side and much less intense than for the other compounds. From the last three samples, the tendency is to have a larger number of Cl^- ions and a lower number of oxygen atoms close to the calcium dication, and from the last 2 samples the corresponding crystal structure shows mostly chloride in the first coordination shell, leading to a much more intense 1s to 4p coupling.

Additional published results focusing on solid samples and presenting different local order around the calcium dication exist. M.E. Fleet and X. Liu[37] and Rebecca et al.[38] collected Ca $L_{2,3}$-edge spectra on e.g. calcite on the one hand, and on synthetic carbonate hydroxylapatite (CHAP) and aragonite on the other hand. A direct observation is that the spectrum we recorded in water solvent at the $L_{2,3}$ edge is very similar to the one of CHAP and somehow comparable with the one of aragonite, whereas the methanol and ethanol solvent cases lead to spectra slightly similar as the calcite one. In the structure of aragonite (water-like in our study), Ca^{2+} is in a 9-fold coordination and from the measurements a weak and positive 10Dq value was obtained. In calcite (alcohol-like in our study), the calcium dication is in an octahedral 6-fold coordination with a geometry close to the ideal O_h symmetry group, whereas for CHAP the structure is more complex and involves two distinct Ca^{2+} having each its own coordination. Despite two different structures, the Ca $L_{2,3}$ X-ray absorption spectra of these last two samples are very similar. Unfortunately, from the CHAP structure the sign of the crystal field cannot be easily obtained

since for a given calcium atom the 10Dq is negative and for the other one this value is positive, but in both cases, the splitting is weak.

Interestingly, L. Brinza et al.,[39] also studied calcite and aragonite by XAFS but at the Ca^{2+} K-edge and from their observations the same conclusion can be drawn: the Ca 1s to 3d pre-edge presents a single structure in aragonite – as for the aqueous solution, and presents a double structure in calcite – as for the ethanol and to a less extend the methanol solvents.

Conclusions:

We have measured the X-ray absorption spectrum of calcium chloride dissolved in three distinct solvents, namely water, methanol and ethanol, at the Ca K and $L_{2,3}$ edges. The interpretation of the observed structures is almost supported by ab-initio quantum chemical calculations assuming a cubic (8-fold) solvent coordination to Ca^{2+}.

At the Ca K-edge, below the 1s ionization threshold: small change of the pre-peak shape as a function of the solvent. One large unresolved structure for water, contrary to ethanol for which an apparent double structure is observed, methanol being an intermediate case. Above Ca1s threshold, the main structure is associated with the 1s to 4p transition. For water solvent there is no obvious shoulder on the low energy side near the threshold, whereas for the two other solvents we observe an extra structure associated with excitonic features having a 4p character.

At the $L_{2,3}$ edge, the X-ray absorption spectra are also solvent dependent. For each spectrum, we observe two groups of peaks associated with the $2p_{1/2,3/2}$ spin-orbit components, each of them being composed of sub-groups of peaks arising from crystal field splitting. These sub-groups

have a main intense 3d t_{2g} peak, preceded by a series of smaller 3d e_g features which are more sensitive to the type of solvent.

Author Information:

Corresponding Author

*E-mail: denis.ceolin@synchrotron-soleil.fr

Acknowledgements:

This work has been partially supported by the Research Network NANOTEC program of the National Nanotechnology Center, NSTDA, Ministry of Higher Education, Science, Research and Innovation, Thailand. Campus France and the PHC SIAM exchange program are acknowledged for financial support (project N° 38282QB).

Data Availability Statement:

The data that support the findings of this study are available from the corresponding author upon reasonable request.

References:

[1] V.-T. Pham and J.L. Fulton, The Journal of Chemical Physics 138, 044201 (2013)

[2] A. Tongraar, J.T.-Thienprasert, S. Rujirawat, S. Limpijumnong, Phys. Chem. Chem. Phys., 12, 10876 (2010),

[3] F.C. Lightstone, E. Schwegler, M. Allesch, F. Gygi, G. Galli, ChemPhysChem 6, 1745 (2005)

[4] F. Jalilehvand, D. Spångberg, P. Lindqvist-Reis, K. Hermansson, I. Persson, M. Sandström, J. Am. Chem. Soc. 123, 431 (2001)

[5] T. Megyes, T. Grósz, T. Radnai, I. Bakó, G. Pálinkás, J. Phys. Chem. A 108, 7261 (2004)

[6] J.L. Fulton, S.M. Heald, Y.S. Badyal, J.M. Simonson, J. Phys. Chem. A 107, 4688 (2003)

[7] J.L. Fulton, Y. Chen, S.M. Heald, M. Balasubramanian, J. Chem. Phys. 125, 094507 (2006)

[8] Y.S. Badyal, A.C. Barnes, G.J. Cuello, J.M. Simonson, J. Phys. Chem. A 108, 11819 (2004)

[9] A.A. Chialvo and J.M. Simonson, J. Chem. Phys. 119, 8052 (2003)

[10] H.-S. Kim, Journal of Molecular Structure (Theochem) 541, 59 (2001)

[11] B. Hesse, M. Salome, H. Castillo-Michel, M. Cotte, B. Fayard, C.J. Sahle, W. De Nolf, J. Hradilova, A. Masic, B. Kanngießer, M. Bohner, P. Varga, K. Raum, S. Schrof, Anal. Chem. 88, 3826 (2016)

[12] D.L. Proffit, T.T. Fister, S. Kim, B. Pan, C. Liao, J.T. Vaughey, J. Electrochem. Soc. 163, A2508 (2016)

[13] T. Hatsui, E. Shigemasa, N. Kosugi, AIP Conf. Proc. 705, 921 (2004)

[14] M. Nagasaka, H. Yuzawa, T. Horigome, N. Kosugi, Journal of Electron Spectroscopy and Related Phenomena 224, 93 (2018)

[15] https://www.slri.or.th/en/bl1-1w.html

[16] K. Ueda, M. Okunishi, H. Chiba, Y. Shimizu, K. Ohmori, Y. Sato, E. Shigemasa, N. Kosugi, Chem. Phys. Lett. 236, 311 (1995)

[17] N. Kosugi and T. Ishida, Chem. Phys. Lett. 329, 138 (2000)

[18] N. Kosugi, J. Electron Spectrosc. 137, 335 (2004)

[19] S. Huzinaga, J. Andzelm, M. Klobukowski, E. Radzio-Andzelm, Y. Sakai, H. Tatewaki, Physical Sciences Data, vol. 16, Elsevier, Amsterdam, 1984

[20] N. Kosugi, H. Kuroda, Chem. Phys. Lett. 74, 490 (1980)

[21] N. Kosugi, Theor. Chim. Acta 72, 149 (1987)

[22] D. Céolin et al. in preparation

[23] V. Martin-Diaconescu, M. Gennari, B. Gerey, E. Tsui, J. Kanady, R. Tran, J. Pécaut, D. Maganas, V. Krewald, E. Gouré, C. Duboc, J. Yano, T. Agapie, M.N. Collomb, S. Debeer, Inorg. Chem. 54, 1283 (2015)

[24] F.E. Sowrey, L.J. Skipper, D.M. Pickup, K.O. Drake, Z.Lin, M.E. Smith, R.J. Newport, PCCP 6, 188 (2004)

[25] N. Kosugi, H. Kondoh, H. Tajima, H. Kuroda, Chemical Physics 135, 149 (1989)

[26] S.J. Naftel, T.K. Sham, Y.M. Yiu, B.W. Yates, J. Synchrotron Rad., 8, 255 (2001)

[27] D. Rieger, F.J. Himpsel, U.O. Karlsson, F.R. McFeely, J.F. Morar, J.A. Yarmoff, Phys. Rev. B, 34, 7295 (1986)

[28] F.J. Himpsel, U.O. Karlsson, J.F. Morar, D. Rieger, J.A. Yarmoff, Phys. Rev. Lett. 56, 1497 (1986)

[29] T. Jiang, K. Koshmak, A. Giglia, A. Banshchikov, N.S. Sokolov, F. Dinelli, R. Capelli, L. Pasquali, J. Phys. Chem. C, 121, 4426 (2017)

[30] C.T. Chen and F. Sette, Comment on "Determination of Interface States for CaF_2/Si(111) from Near-Edge X-Ray-Absorption Measurements", Phys. Rev. Lett. 60 (1988) 160

[31] F.M.F. de Groot, J.C. Fuggle, B.T. Thole, G.A. Sawatzky, Phys. Rev. B, 41, 928 (1990)

[32] F.J. Himpsel, U.O. Karlsson, A.B. McLean, L.J. Terminello, F.M.F. de Groot, M. Abbate, J.C. Fuggle, J.A. Yarmoff, B.T. Thole, G.A. Sawatzky, Phys. Rev. B 43, 6899 (1991)

[33] F.J. Himpsel, U.O. Karlsson, J.F. Morar, D. Rieger, J.A. Yarmoff, Reply, Phys. Rev. Lett. 60 (1988) 161

[34] P. Krüger and C.R. Natoli, Phys. Rev. B 70, 245120 (2004)

[35] K. Ogasawara, T. Iwata, Y. Koyama, T. Ishii, I. Tanaka, H. Adachi, Phys. Rev. B 64, 115413 (2001)

[36] P.S. Miedema, H. Ikeno, F.M.F. de Groot, J. Phys.: Condens. Matter 23, 145501 (2011)

[37] M.E. Fleet, X. Liu, Am. Mineral. 94, 1235 (2009)

[38] Rebecca A. Metzler and Peter Rez, J. Phys. Chem. B 118, 6758 (2014)

[39] L. Brinza, P.F. Schofield, M.E. Hodson, S. Weller, K. Ignatyev, K. Geraki, P.D. Quinn, J.F.W. Mosselmans, J. Synchrotron Rad. 21, 235 (2014)